*Journal of Edge Computing*, **2023**, 2(1), pp. 64-83 https://doi.org/10.55056/jec.627

# Model of an automated biotechnical system for analyzing pulseograms as a kind of edge devices

*Tetiana M.* Nikitchuk[1], *Oleksandr V.* Andreiev[1], *Oksana L.* Korenivska[1] and *Mykhailo G.* Medvediev[2]

[1]*Zhytomyr Polytechnic State University, 103 Chudnivsyka Str., Zhytomyr, 10005, Ukraine*
[2]*ADA University, School of Information Technologies and Engineering, 61 Ahmadbay Agha-Oglu Str., Baku, AZ1008, Azerbaijan*

**Abstract.** The rapid development of computer biometrics over the past 2-3 decades is largely due to the development and widespread introduction into clinical practice of new methods of studying human body health, including pulse methods. It is possible to judge changes in hemodynamic characteristics, heart rate, and blood flow rate in the studied part of the body based on the parameters of the pulse wave signal. At the same time, the physical processes of the formation of the pulse wave shape have not been fully studied, although the number of biophysical models of blood circulation is quite significant. The development of such a model will allow us to effectively apply modern developments in digital signal processing to the pulse wave and increase its diagnostic value. A qualitative model of pulse signal can be entrusted to the development of the base unit of the biotechnical system as a type of edge device. The work is devoted to the improvement of methods of rapid diagnosis of the cardiovascular system based on the analysis of model pulse-grams. An adequate mathematical model of the pulse wave, which corresponds to real pulse signals in different states of the human body and contains mathematical relationships between the main parameters of pulse-grams, has been refined. The algorithm of express diagnostics with the established criteria of the analysis of pulsograms is offered[1].

**Keywords:** edge device, model, pulse signal, pulse waveform, phase plane, phase portrait

## 1. Introduction

The rapid development of computer biometrics over the past 2-3 decades is largely due to the development and widespread introduction into clinical practice of new methods of studying human body health, including pulse methods. It is possible to judge changes in hemodynamic characteristics, heart rate, and blood flow rate in the studied part of the body based on the parameters of the pulse wave signal. At the same time, the physical processes of the formation of the pulse wave shape have not been fully studied, although the number of biophysical models of blood circulation is quite significant. However, none of them meets all the requirements for models of the pulse signal in terms of rapid and pulse diagnostics, namely:

- match with the real signal in all areas of blood circulation;

[1]This article is an extended version of a previous study [8].

tnikitchuk@ukr.net (T. M. Nikitchuk); oleks.andreyev@gmail.com (O. V. Andreiev); o.l.korenivska@gmail.com (O. L. Korenivska); miserablewisdom@ukr.net (M. G. Medvediev)
0000-0002-9068-931X (T. M. Nikitchuk); 0000-0002-2601-1491 (O. V. Andreiev); 0000-0002-3735-7690 (O. L. Korenivska); 0000-0002-3884-1118 (M. G. Medvediev)

- not only the form reproduction but also the explanation of the pulse wave genesis;
- description of the circulatory system activity in the diastolic phase;
- presence of mathematical equations that coordinate the basic parameters of blood flow;
- relative simplicity of interpretation with sufficient information value.

The development of such a model will allow us to effectively apply modern developments in digital signal processing to the pulse wave and increase its diagnostic value. A qualitative model of pulse signal can be entrusted to the development of the base unit of the biotechnical system as a type of edge device (figure 1).

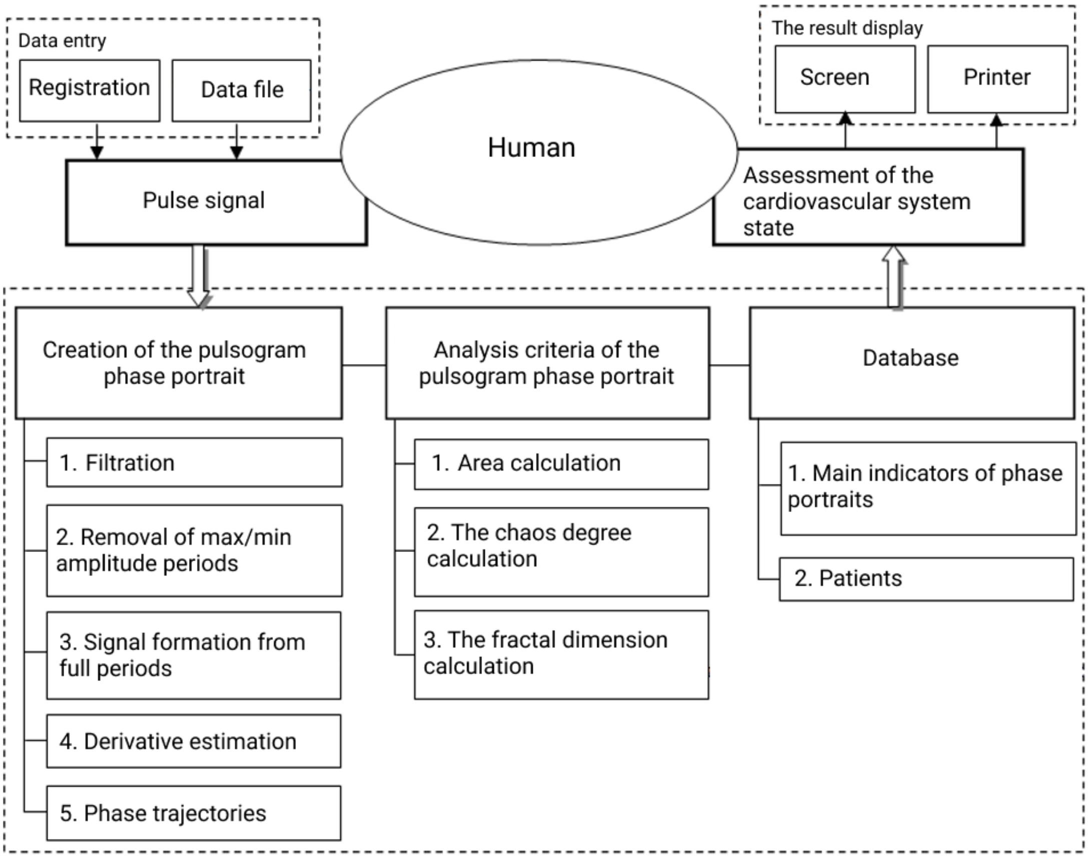


**Figure 1:** Block diagram of the automated biotechnical system of pulsegram analysis [8].

## 2. Theoretical background

An edge device is a peripheral device capable of forwarding packets between traditional interfaces (e.g. Ethernet, Token Ring, etc.) and ATM based on channel or network layer information. However, it is not involved in any routing protocol on the network.

According to Nan et al. [6], a large amount of patient data can be analyzed on the periphery. Next, it needs to be transformed. Only after that, the relevant data can be sent to the cloud. According to the scientists, “peripheral medical imaging eliminates latency and dependence on cloud computing resources, as well as reduces the patient’s digital footprint by limiting the number of systems that have access to data” [6].

Krishnasamy, Varrette and Mucciardi [4] describes how Edge Computing is used in the healthcare system (figure 2). Scientists claim that edge computing makes the modern health care system more critical and sensitive by reducing the time spent on data transmission compared to the autonomous cloud system [4].

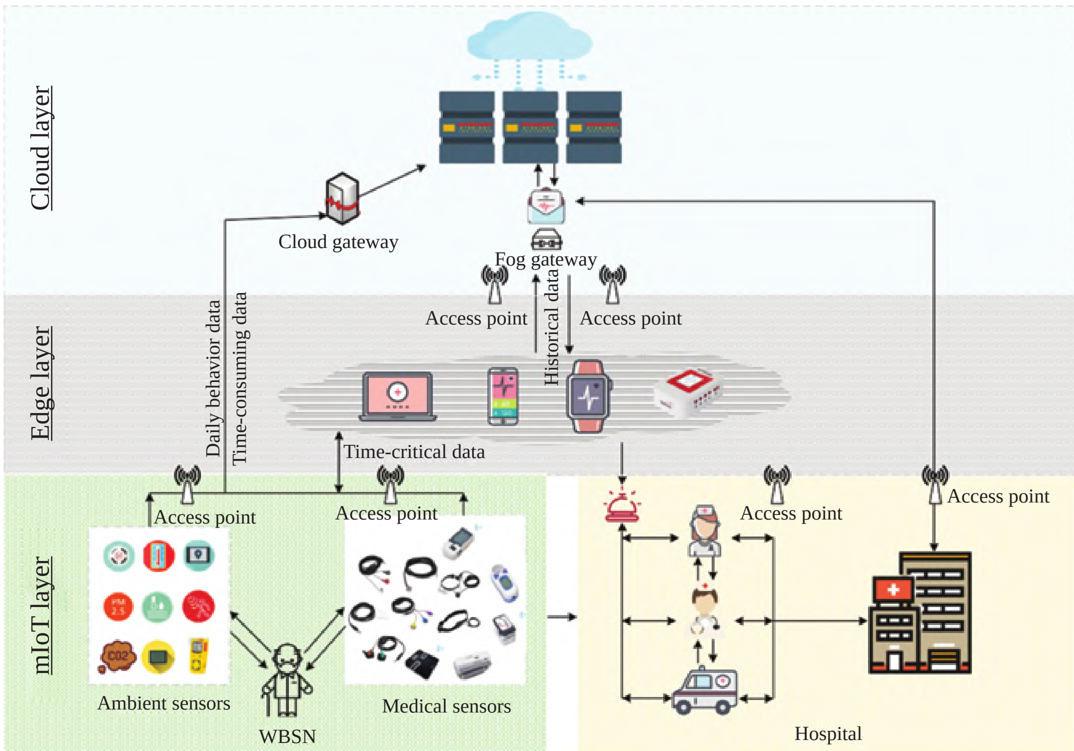


**Figure 2:** Edge Computing in Healthcare [4].

Pazienza et al. [10] discribed the eLifeCare platform uses AI on the Edge level (figure 3). They say that the platform acts as an alert system using early warning indicators (some forms of edge devices) [10].

Quy et al. [11] consider the architecture of fog-based applications. They note that such an architecture consists of three layers: Thing Layer, Fog Layer, and Cloud Layer. In particular, the Thing Layer level includes end-user devices (edge devices) (figure 4). Those are Arduino motherboards, IoT devices, sensors, body data collection tools (e.g. blood pressure, heart rate, glucose), and so on [11].

Nikitchuk et al. [9] suggest an architecture for edge devices for diagnostics of students’ physical condition. The biotechnical system can then be built based on their research.

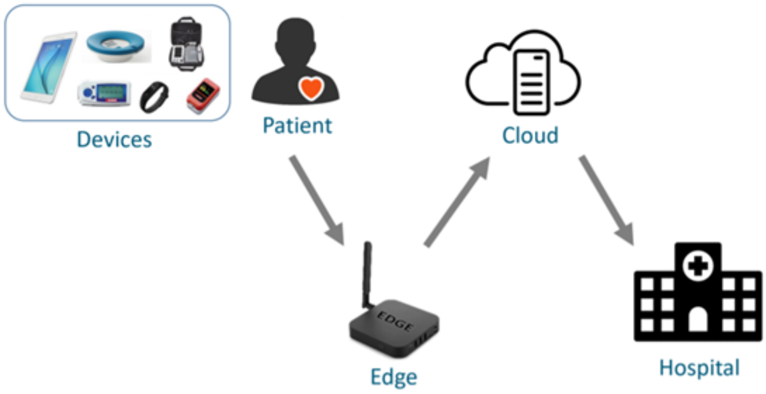


**Figure 3:** Healthcare Scenario in AAL [10].

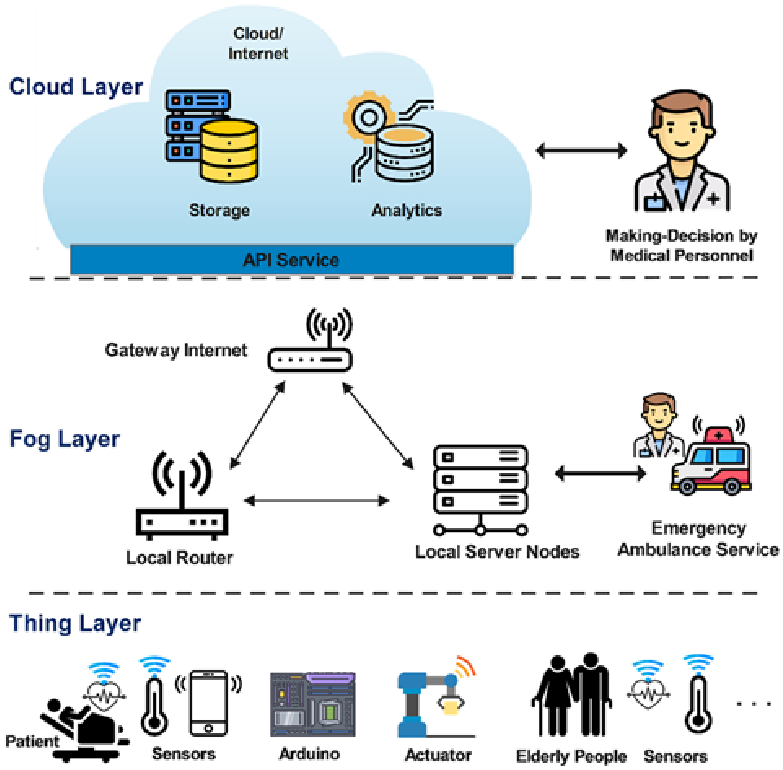


**Figure 4:** Fog-based application architecture [11].

This article aims to develop a mathematical model of the pulse wave, which will correspond to the real pulse signals for certain types of pulsations in the circulatory system, contain mathematical relationships between basic parameters of pulse-grams and will be the basis of a biotechnical system to improve rapid diagnostics of the cardiovascular system.

## 3. Research methodology

In the methodological aspect, the study of such complex systems as physiological is carried out on adequate mathematical models using modern computer technology. Data analysis includes:

(a) mathematical description, modeling, and parameterization of data;
(b) data classification by diagnostic categories to further automate the conclusion;
(c) graphic or other visual presentation of the results for the diagnostician.

In the first stage, the selected and/or improved model is analyzed and calculated on a PC (which is a model computational experiment). It should be kept in mind that modeling is a process of studying a phenomenon with the help of mathematical equations. The model is just a simplified description of real phenomena and processes. Therefore, the results obtained by computer simulation need further confirmation (for example, by conducting a clinical experiment).

The second stage is the calculation of the object's characteristics, the definition of diagnostic criteria, and the creation of an identification box (expert system) to automate the conclusion in further clinical trials.

An analysis of modern methods and tools has established [7] that classification by the characteristics of a single pulse wave and classification at an interval of 3-5 periods are not sufficiently informative, since they do not take into account the variability of cardiovascular system indicators expressed in fluctuations in the characteristics of pulseograms over a long interval, which corresponds to the procedure of recording pulse waves for 3-5 minutes.

Therefore, we propose a classification [7] based on the variability of pulseogram characteristics throughout the diagnostic procedure.

To study the dynamics of the cardiovascular system and obtain a set of diagnostic criteria for the analysis of pulse waves over long time intervals, it is recommended to use the methods and techniques of fractal analysis as those that allow to identify the self-similarity and regularity of time sequences. In particular, the phase plane method can be used to quantitatively describe pulse waveforms over a long time interval. The effectiveness of this method lies primarily in the fact that with various changes in the heart rhythm, in case of cardiovascular system dysfunctions, not only the sequence of periods changes but also the rate of their change in time. Therefore, a differentiated pulse signal inevitably contains additional information about the state of the subject's cardiovascular system.

To quantify the obtained trajectories of pulse signals in the phase plane (phase portraits of pulseograms), it is possible to use such indicators as the area of the phase portrait, the degree of portrait chaos, and the fractal dimension of the phase portrait.

At the last stage of computer analysis, the conclusion is performed and the result is displayed in visual form (monitor screen) and/or graphical representation for the diagnostician.

The algorithm for automated inference about the state of a physiological object by creating a classification base (identification box) with the use of model data is shown in figure 5.

Each of the listed stages of data processing and process analysis in a certain period quickly improves, moving to a higher quality level almost abruptly. For example, acquainting a doctor with a diagnosis (conclusion about the state of the biological system), set by the computer automatically, helps to increase the accuracy of the final diagnostic conclusion [7].

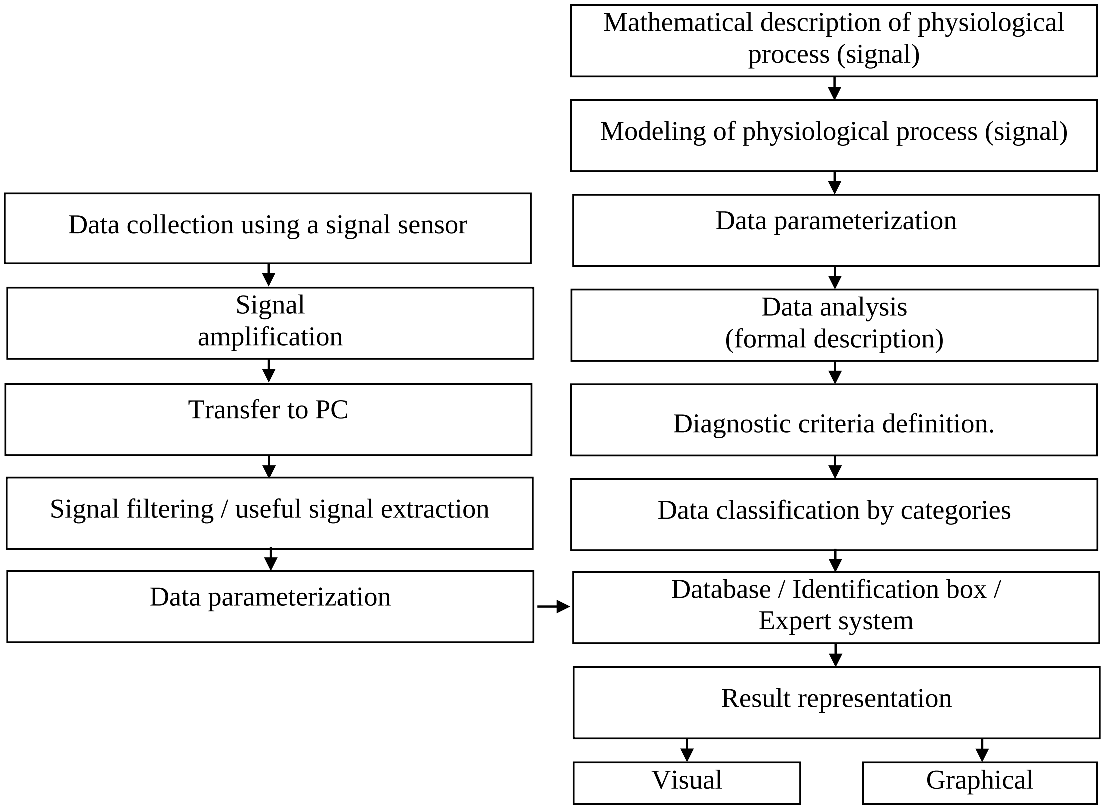


**Figure 5:** Algorithm for conducting research and automatic inference about the state of a physiological object using model data.

## 4. Results

The rapid development of computer biometrics over the past 2-3 decades is largely due to the development and widespread introduction of new, including pulse, methods of studying the state of health of the human body into clinical practice. Based on the parameters of the pulse wave signal, it is possible to judge changes in hemodynamic characteristics, heart rhythm, and blood filling rate in the part of the body under study. At the same time, the physical processes of pulse wave formation are not yet fully understood.

The number of biophysical models of blood circulation is quite significant. At the same time, none of them satisfies all the requirements for pulse signal models in terms of express and pulse diagnostics:

- coincidence with the real signal in all parts of the circulation;
- reproduction of not only the shape but also explanation of the genesis of the pulse wave;
- description of the circulatory system in the diastolic phase;
- availability of mathematical equations that coordinate the main parameters of blood flow;
- relative ease of interpretation with sufficient information value.

When comparing the vast majority of models and the real signal, discrepancies arise, sometimes significant ones, which cannot be explained by the accompanying factors of pulse wave registration. That is, these are not distortions in the signal caused by the imposition of noise and artifacts, but rather inaccuracies in the representation of blood flow pulsations. Most often, such inaccuracies arise when trying to apply the model to vessels much further away from the heart than the aorta, the so-called peripheral bloodstream. Nevertheless, several models successfully describe individual parts of the circulatory system. However, these models are of theoretical rather than practical value – they attempt to take into account all possible processes in and around the vessel, while the emphasis is not on simple relationships of the main parameters or such relationships are difficult to implement.

Based on the analysis of existing biophysical models of blood circulation [1–3, 5], it follows that none of the existing models reflects all elements of the pulse wave accurately enough. Therefore, they cannot be used in developing new methods for analyzing pulse signals in particular and the cardiovascular system in general. However, the harmonious model of blood circulation and the model of active diastole can be considered as those that accurately reflect the genesis of pulse waves. They are quite simple and are partially confirmed by practical results [5].

Based on these two models, a mathematical model of blood circulation was developed in [3, 5]. It was called harmonic three-phase. According to this model, the activity of the circulatory system is considered to be three-phase, i.e. the pulse signal is formed by three components: systolic, dichroic, and presystolic [5]:

$$p_{gen} = p_s + p_d + p_{presyst}. \tag{1}$$

The systolic component occurs as a result of the release of blood from the left atrium into the aorta. It is described by the harmonic model of circulation as follows

$$p_s = p_0 exp[-\chi^l] cos\omega \left(t - \frac{1}{v}\right). \tag{2}$$

When analyzing the pulse waveform locally, you can set local values of blood flow parameters. Considering the brachial artery as the area of sensor overlap, and taking into account the ratio

$$p_o^{place} = p_0 \cdot exp\left[-\chi^l\right], \tag{3}$$

the systolic component in the brachial artery can be represented by the following equation:

$$p_s^{place} = p_0^{place} \cdot cos\omega \left(t - \frac{1}{v}\right). \tag{4}$$

The dicrotic component, which is part of the total signal, is associated with the active activity of the venous system. From practical clinical results, the general characteristics of the dicrotic component and their approximate correlation with similar parameters of the systolic component are known. Based on these data, the equation of the dicrotic component in the brachial artery was developed:

$$p_d^{place} = p_0^{\prime place} \cdot \left| sin\omega^{\prime} \left( t - \frac{1}{v^{\prime}} + \varphi^{\prime} \right) \right|, \tag{5}$$

where $p_0^{\prime place}$ – is the amplitude of the dicrotic wave; $\omega^{\prime}$ – is the circular frequency of the dicrotic wave; $v^{\prime}$ – the velocity of the dicrotic component of the pulse wave; $\varphi^{\prime}$ – time delay between systolic and dicrotic components.

Since most arteries (except for the aorta and carotid artery) and veins are muscle-type vessels, their pulse wave propagation properties are the same. Consequently, the propagation speed of the dicrotic wave is $v = 6.8$ m/s for the same category of people. The distance from the heart, is included in the equation as a parameter $l = 0.4$ m. Since only a positive half-wave is used as a dicrotic component, to ensure synchronization in signal formation, the circular frequency of the dicrotic wave will be half that of the systolic wave frequency, $\omega^{\prime} = 2/\omega = 3.3$ rad/s (the numerical value is valid for the specified category).

Regarding the delay in time of occurrence, the dicrotic wave begins at the moment of the beginning of the systolic wave decline, that is, immediately after its maximum, therefore, for this category of patients it is $\varphi^{\prime} = 0.06 - 0.12$ s.

The presystolic component occurs due to the release of blood from the left ventricle into the atrium. As in the case of the dicrotic component, the presence of valves leads to the fact that the presystolic component is only a positive half-sine wave. Based on general ideas about the formation of this component, its equation in the brachial artery is as follows:

$$p_{presyst}^{place} = p_0^{\prime\prime place} \cdot \left| sin\omega^{\prime\prime} \left( t - \frac{1}{v^{\prime\prime}} + \varphi^{\prime\prime} \right) \right|, \tag{6}$$

where $p_0^{\prime\prime place}$ – is the amplitude of the presystolic wave; $\omega^{\prime\prime}$ – is the circular frequency of the presystolic wave; $v^{\prime\prime}$ – the velocity of the presystolic component of the pulse wave; $\varphi^{\prime\prime}$ – time delay between systolic and presystolic components.

The relationship between the amplitudes of the presystolic and dicrotic waves $p_0^{\prime\prime place} \approx p_0^{\prime place}$. Since only the positive half-wave is involved in the formation of the contour, its frequency will coincide with the frequency of the dicrotic wave $\omega^{\prime\prime} = \omega^{\prime} = \frac{\omega}{2} = 3.30$, the propagation speed and distance from the heart for all these components are the same, as evidenced by the uniformity of the contour within a particular area of the blood flow. The phase shift between the systolic and presystolic waves can be found based on the analysis of real pulseograms. According to the results of the analysis presented in [7], the presystolic wave has a maximum at a distance of 0.1 to 0.3 s from the top of the systolic wave, and the presystolic wave appears earlier. The shorter the time delay, the more pronounced the presystolic component. Since no presystolic peak is observed on the brachial plethysmogram, we take $\varphi^{\prime\prime} \approx 0.3$ s.

Taking into account the pressure around the artery to be recorded, the change in pulsations in the brachial artery based on equations (5)-(6) can be written

$$p^{place} = p_a^{place} + p_s^{place} + p_d^{place} + p_{presyst}^{place}. \tag{7}$$

The model is a one-dimensional signal, the position of the extremes and characteristic points of which corresponds to a human pulse wave without pathologies of the cardiovascular system.

The duration is chosen based on several heartbeats. In terms of the data set, this curve is an array of 600 discrete points, which corresponds to a signal with a sampling frequency of 100 Hz (the value of the pressure in the model is calculated at intervals of 0.01 sec.)

The model analysis procedure gives an idea of the effectiveness and feasibility of applying appropriate software and algorithms to the real signal. A fragment of the model is graphically shown in figure 6.

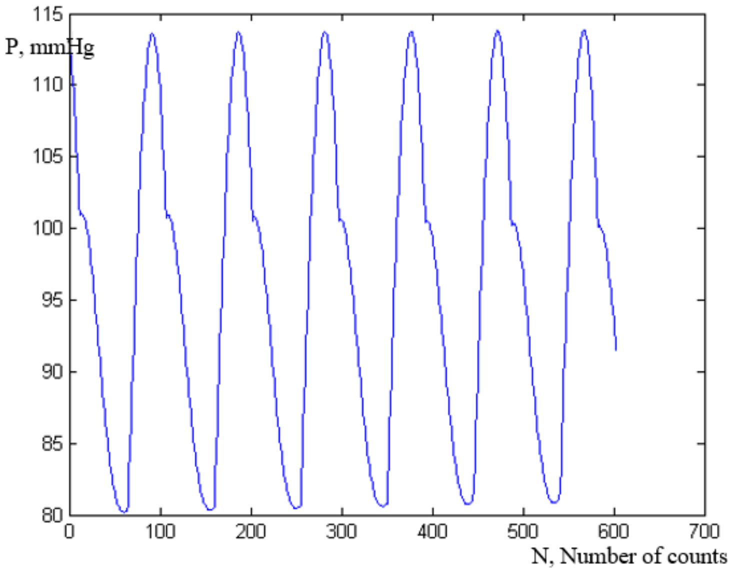


**Figure 6:** A fragment of the model signal.

Assume that the real and mathematically described pulse signals are identical [7]. That is, the pulse wave mathematical equation can be developed for the selected 6 types of pulse presented in the classification system based on the variability of the pulsegram characteristics during the diagnostic procedure [7], with the definition of the corresponding dysfunctions of the cardiovascular system.

General view of the mathematical equation of the pulse wave

$$p = p_a + p_0 \cdot \cos\omega\left(t - \frac{l}{v}\right) + p_0' \cdot \left|\sin\omega'\left(t - \frac{l}{v} + \varphi'\right)\right| + 1.5 \cdot p_0'' \cdot \left|\sin\omega''\left(t - \frac{l}{v} + \varphi''\right)\right| \quad (8)$$

or, considering $\omega'' = \omega' = \frac{\omega}{2} = 3.30$ and $p_0'' \approx p_0'$,

$$p = p_a + p_0\left[\cos\omega\left(t - \frac{l}{v}\right) + \frac{3}{2}\left(\left|\sin\frac{\omega}{2}\left(t - \frac{l}{v} + \varphi'\right)\right| + \left|\sin\frac{\omega}{2}\left(t - \frac{l}{v} + \varphi''\right)\right|\right)\right] \quad (9)$$

Taking into account the nominal parameters of blood flow for the category of people with the same type of anthropometric and physiological parameters, without obvious dysfunctions of the heart, the mathematical equation for the pulse signal of "even pulse"

$$p_{even} = 50 + 18.75 \cdot \cos 6.61 \left(t - \frac{0.06}{6.8}\right) + 28.13 \cdot \left|\sin 3.30 \left(t - \frac{0.06}{6.8} + 0.12\right)\right| + \\ +28.13 \cdot \left|\sin 3.30 \left(t - \frac{0.06}{6.8} - 0.30\right)\right| = 50 + 18.75 \cdot \cos 6.61 \left(t - \frac{0.06}{6.8}\right) + \\ +28.13 \cdot |\sin 3.30(t + 0.11)| + 28.13 \cdot |\sin 3.30(t + 0.29)| \quad (10)$$

According to the equation, computer simulation of the signal "even pulse" was conducted (figure 7).

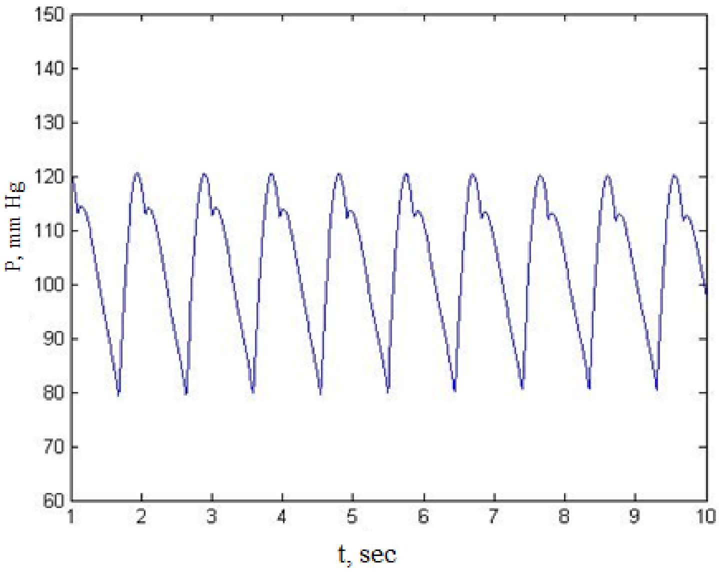


**Figure 7:** Model signal of "even" pulse.

Equation for pulse signal type "uneven pulse":

$$p_{uneven} = 50 + 18.75 \cdot \cos 6.61 \left(t - \frac{0.06}{6.8}\right) + 28.13 \cdot \left|\sin 3.30 \left(t - \frac{0.06}{6.8} + 0.15\right)\right| + \\ +28.13 \cdot \left|\sin 3.30 \left(t - \frac{0.06}{6.8} + 0.22\right)\right| = 50...55 + 18.75 \cdot \cos 6.61(t - 0.0088) + \\ +28.13 \cdot |\sin 3.30(t + 0.14)| + 28.13 \cdot |\sin 3.30(t + 0.21)| \quad (11)$$

By changing the hemodynamic parameters included in the equation of the pulse wave, a graph of the "uneven" type of pulse was obtained by computer simulation (figure 8).

The equation for pulse signal type "high pulse"

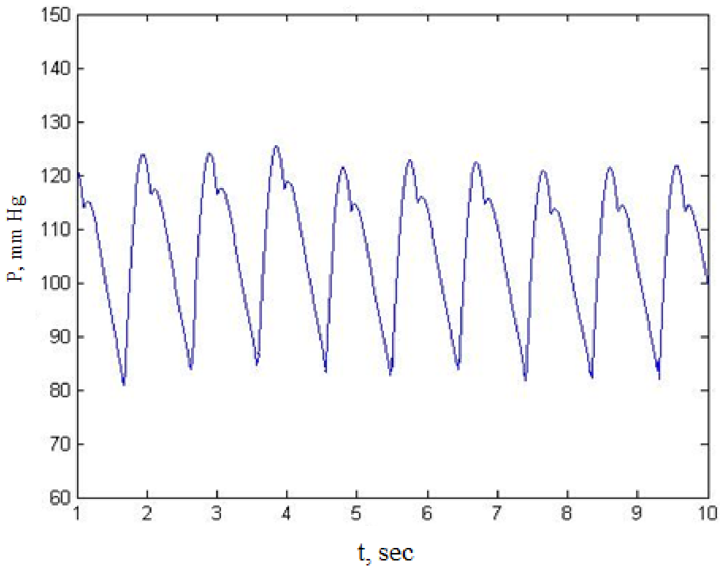


**Figure 8:** Model signal of "uneven" pulse.

$$p_{high} = 60 + 18.75 \cdot \cos 6.61 \left(t - \frac{0.06}{6.8}\right) + 28.13 \cdot \left|\sin 3.30 \left(t - \frac{0.06}{6.8} + 0.09\right)\right| + \\ +28.13 \cdot \left|\sin 3.30 \left(t - \frac{0.06}{6.8} + 0.32\right)\right| = 60 + 22.5 \cdot \cos 6.61(t - 0.0088) + \\ +34.6 \cdot |\sin 3.30(t + 0.08)| + 34.6 \cdot |\sin 3.30(t + 0.31)| \tag{12}$$

The graphic result of the computer simulation of the "high" pulse is shown below (figure 9). The equation for the type of pulse signal "low pulse", is shown in figure 10.

$$p_{low} = 45 + 9.4 \cdot \cos 6.61 \left(t - \frac{0.06}{6.8}\right) + 33.8 \cdot \left|\sin 3.30 \left(t - \frac{0.06}{6.8} + 0.9\right)\right| + \\ +33.8 \cdot \left|\sin 3.30 \left(t - \frac{0.06}{6.8} + 0.2\right)\right| = 45 + 9.4 \cdot \cos 6.61(t - 0.0088) + \\ +33.8 \cdot |\sin 3.30(t + 0.89)| + 33.8 \cdot |\sin 3.30(t + 0.19)| \tag{13}$$

The type of pulse "fast" is described by the equation:

$$p_{fast} = 75 + 45.13 \cdot \cos 6.61 \left(t - \frac{0.06}{6.8}\right) + 28.13 \cdot \left|\sin 3.30 \left(t - \frac{0.06}{6.8} + 0.135\right)\right| + \\ +33.8 \cdot \left|\sin 3.30 \left(t - \frac{0.06}{6.8} + 0.06\right)\right| = 75 + 43.13 \cdot \cos 6.61(t - 0.0088) + \\ +33.8 \cdot |\sin 3.30(t + 0.126)| + 33.8 \cdot |\sin 3.30(t + 0.05)| \tag{14}$$

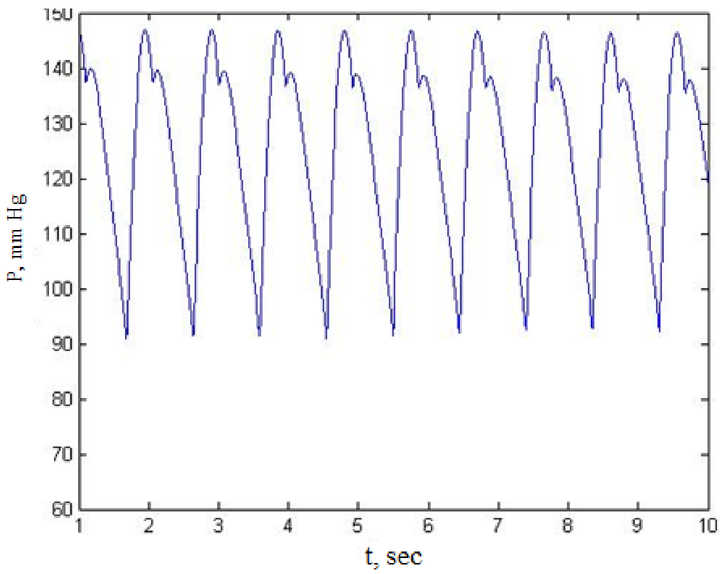


**Figure 9:** Model signal of “high” pulse.

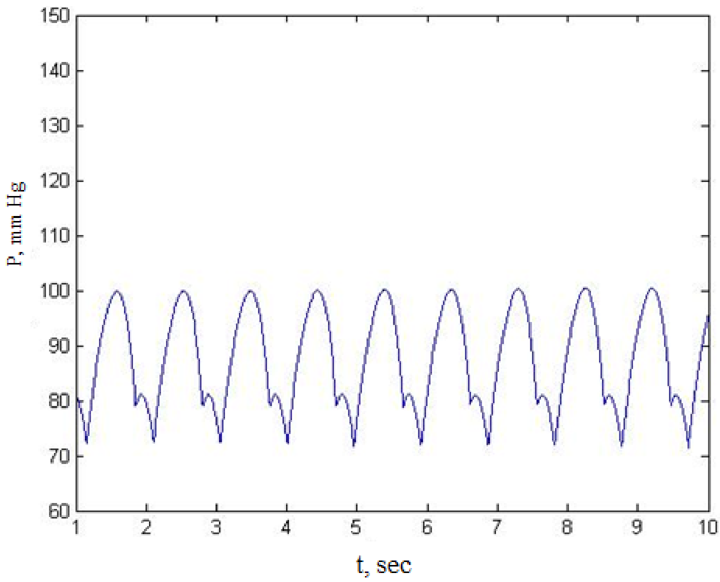


**Figure 10:** Model signal of “low” pulse.

The graphic result of the computer simulation of the “fast” pulse is shown in the figure 11.

By changing the hemodynamic parameters included in the equation of the pulse wave, the equation and the graph of the “slow” type of pulsations are obtained (figure 12).

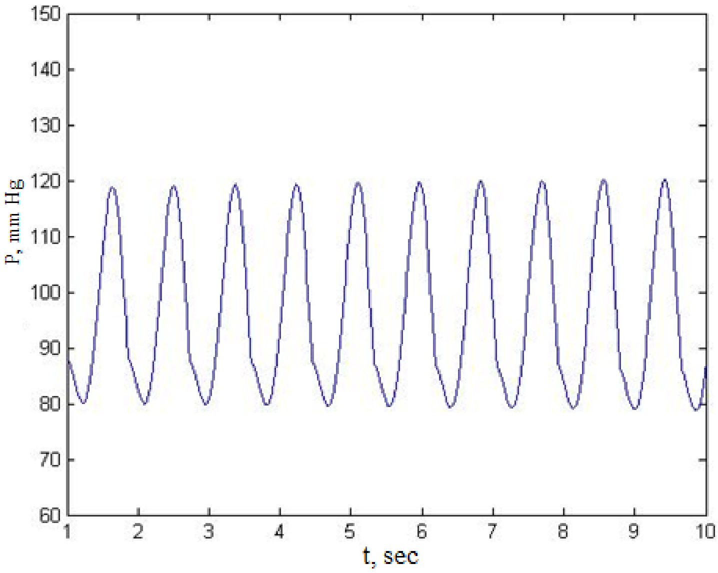


**Figure 11:** Model signal of "fast" pulse.

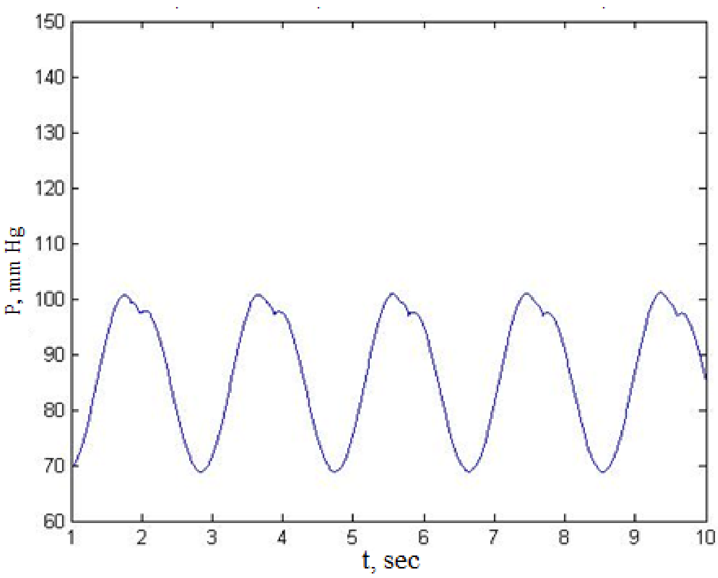


**Figure 12:** Model signal of "slow" pulse.

$$\begin{gathered}p_{slow} = 80 + 20.63 \cdot \cos 6.61 \left(t - \frac{0.06}{6.8}\right) + 16.88 \cdot \left|\sin 3.30 \left(t - \frac{0.06}{6.8} + 0.075\right)\right| + \\ +16.88 \cdot \left|\sin 3.30 \left(t - \frac{0.06}{6.8} + 0.055\right)\right| = 80 + 20.63 \cdot \cos 6.61(t - 0.0088) + \\ +16.88 \cdot |\sin 3.30(t + 0.066)| + 16.88 \cdot |\sin 3.30(t + 0.046)|\end{gathered} \tag{15}$$

The obtained mathematical equations of signals for six types of pulse are presented in the phase plane. The numerical indicators of phase portraits of pulse-grams are investigated (PPP) to determine the criteria for rapid diagnosis.

To carry out express diagnostics on pulsegrams, it is necessary to receive indicators on which the conclusion will be automatically received. It is expedient to plow with the phase plane method substantiated in [7].

According to [7], phase portrait can be formed by putting on one axis the signal itself $p = x(t)$, and on the other one – its derivative $x(t) = p(t)$ (figure 13).

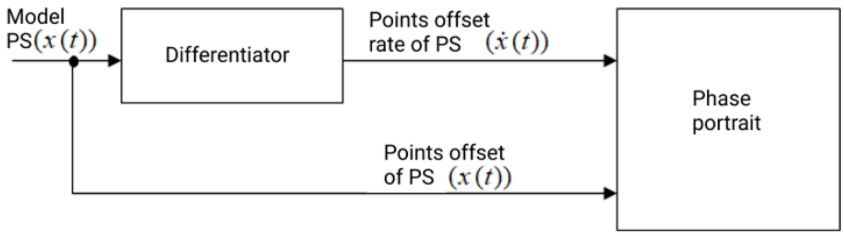


**Figure 13:** Algorithm for forming a phase portrait of a model pulse signal.

Equations ((3) – (8)) are differentiated and the corresponding ones are obtained $x(t) = p(t)$ for each type of pulse. The visualization of the phase trajectory of the pulsegram periods in the coordinates $p - \frac{dp}{dt}$, corresponding to the coordinates $x - y$, is presented in figures 14, 15, 16, 17, 18, 19.

To quantify the trajectories in the phase plane in [7] the following indicators are considered:

- area of the phase portrait $S$ – the number of occupied cells in the plane;
- degree of chaos $Sh$;
- fractal dimension (maximum length (diameter) of the phase portrait) $D$.

The literature sources show the range of changes in the pulse wave, which allowed to obtain sets of curves according to equations (3) – (8) for each type of pulse. Pulse signals have been

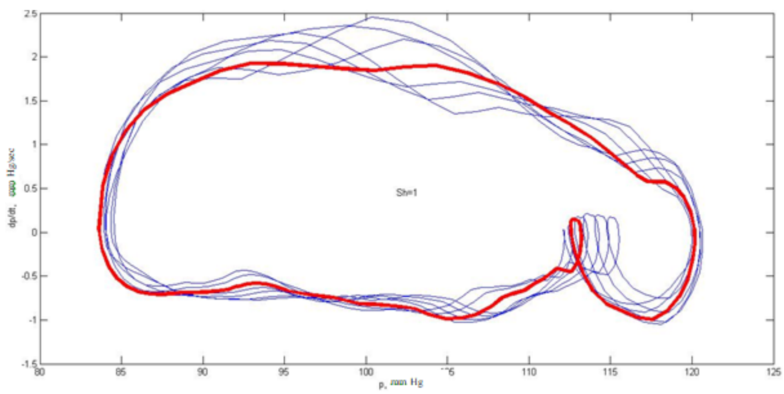

**Figure 14:** Phase portrait of “even” pulse.

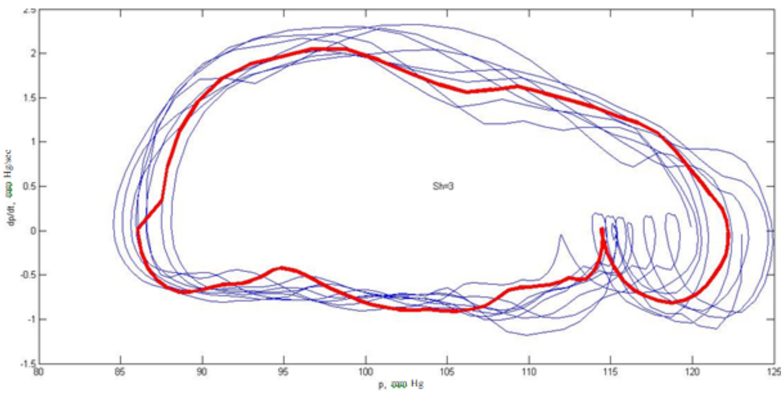


**Figure 15:** Phase portrait of “uneven” pulse.

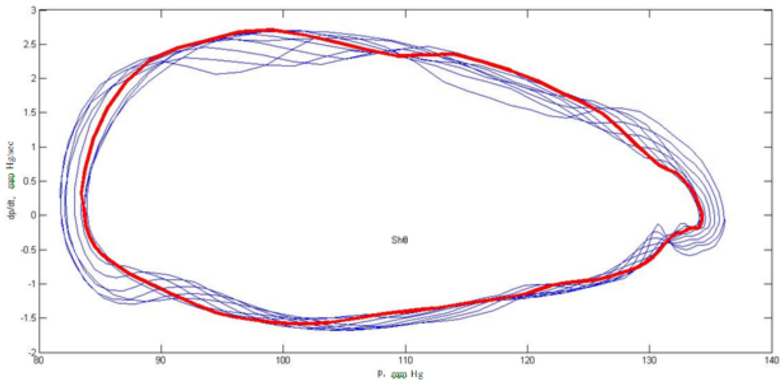


**Figure 16:** Phase portrait of “high” pulse.

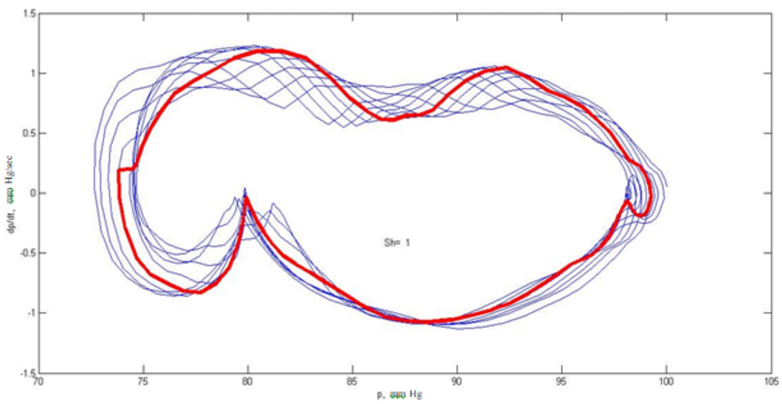


**Figure 17:** Phase portrait of “low” pulse.

presented in the phase plane and their phase portraits have been obtained, according to which the values of PPP characteristics have been calculated (tables 1 and 2).

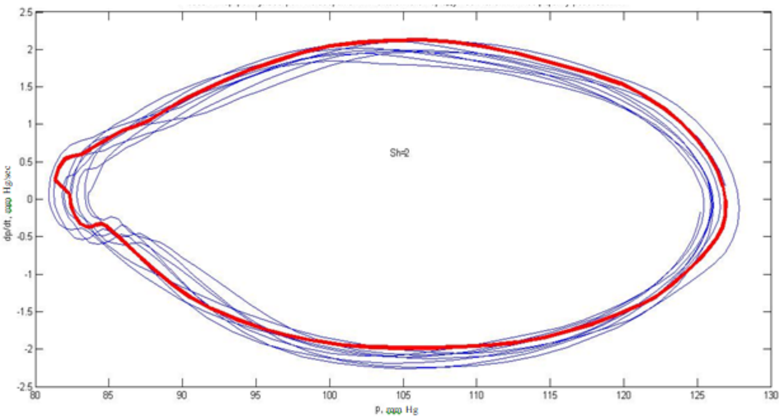


**Figure 18:** Phase portrait of “fast” pulse.

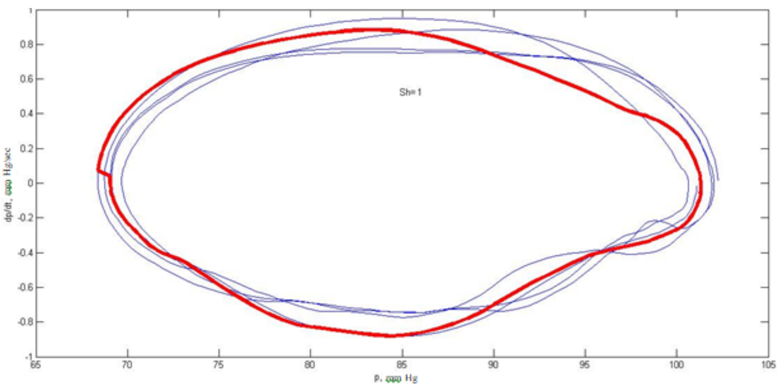


**Figure 19:** Phase portrait of “slow” pulse.

**Table 1**
Numerical values of PPP indicators (“even”, “uneven”, “slow”).

| | Pulse type | | | | | | | | |
|---|---|---|---|---|---|---|---|---|---|
| | “even” | | | “uneven” | | | “slow” | | |
| № | Sh | S | D | Sh | S | D | Sh | S | D |
| 1 | 0.6002 | 666290 | 36.5302 | 2.5924 | 701640 | 36.1376 | 1.0931 | 711620 | 32.9156 |
| 2 | 0.5901 | 669990 | 36.9108 | 2.5601 | 700090 | 35.0056 | 1.0865 | 712900 | 31.9527 |
| 3 | 0.5952 | 670000 | 36.5934 | 2.5333 | 700700 | 35.0000 | 1.0876 | 713660 | 32.0095 |
| 4 | 0.6302 | 668080 | 38.7224 | 2.5599 | 698730 | 35.0006 | 1.0565 | 714590 | 34.7889 |
| 5 | 0.6299 | 662390 | 38.0076 | 2.5436 | 693070 | 35.1551 | 1.0467 | 713050 | 33.4562 |
| 6 | 0.6234 | 660720 | 39.0867 | 2.5502 | 697540 | 35.1456 | 1.0564 | 719800 | 33.0845 |
| 7 | 0.6301 | 659890 | 37.00765 | 2.5101 | 698760 | 35.1305 | 1.0922 | 718540 | 33.789 |
| 8 | 0.6345 | 661730 | 37.6908 | 2.3678 | 690740 | 35.1809 | 1.0928 | 722300 | 34.7655 |
| 9 | 0.6149 | 663420 | 37.2829 | 2.3658 | 689020 | 35.6006 | 1.0205 | 720560 | 33.0098 |
| 10 | 0.6178 | 663980 | 39.11762 | 2.2201 | 685140 | 35.5972 | 1.0198 | 726770 | 34.7733 |

**Table 2**
Numerical values of PPP indicators ("fast", "high", "low").

| | Pulse type | | | | | | | | |
|---|---|---|---|---|---|---|---|---|---|
| | "fast" | | | "high" | | | "low" | | |
| № | Sh | S | D | Sh | S | D | Sh | S | D |
| 1 | 1.5937 | 657740 | 45.5758 | 0.4924 | 710170 | 50.8056 | 0.879 | 783990 | 25.4254 |
| 2 | 1.5003 | 639070 | 45.0995 | 0.506 | 709060 | 50.72135 | 0.9201 | 784060 | 24.43862 |
| 3 | 1.5504 | 649080 | 47.856 | 0.5605 | 706800 | 51.275 | 0.9056 | 783400 | 23.7623 |
| 4 | 1.6980 | 650720 | 47.9008 | 0.5567 | 709570 | 54.8769 | 0.8069 | 783650 | 22.9876 |
| 5 | 1.4280 | 636070 | 46.0405 | 0.5501 | 705010 | 54.623 | 0.8878 | 784520 | 22.1687 |
| 6 | 1.4408 | 641890 | 46.0667 | 0.5598 | 705250 | 51.0432 | 0.8974 | 780040 | 21.7986 |
| 7 | 1.6202 | 643950 | 48.0005 | 0.5344 | 705440 | 53.7634 | 0.8834 | 775400 | 25.1278 |
| 8 | 1.4490 | 651380 | 47.9623 | 0.5201 | 706800 | 54.978 | 0.8001 | 776920 | 25.786 |
| 9 | 1.4208 | 657060 | 47.9405 | 0.5143 | 707020 | 54.0065 | 0.8567 | 776050 | 20.987 |
| 10 | 1.4187 | 634990 | 48.0018 | 0.5104 | 705920 | 51.68788 | 0.8444 | 774700 | 19.28445 |

Using the methods of mathematical statistics, the range of values $A_{k_j}$, where $j_k$ – pulse type with $k$-th PPP indicator, $j = \overline{1,n}$, $n = 6$, $k = \overline{1,h}$, $h = 3$, are defined as the maximum value $A_{max}$ and minimum value $A_{min}$ within each pulse type

$$A_{k_j} = A_{max}...A_{min} \tag{16}$$

The results of the calculation are shown in tables 3 and 4.

That is, the pulse type will be determined as

$$y_j = \begin{cases} A_{Sh}, & A_{minSh} \leq A_{Sh} \leq A_{maxSh} \\ A_S, & A_{minS} \leq A_S \leq A_{maxS} \\ A_D, & A_{minD} \leq A_D \leq A_{maxD} \end{cases} \tag{17}$$

where $y_j$– inference $y$ of a system regarding the pulse type $j$, $j = \overline{1,n}$, $n = 6$.

Then, the block diagram of the algorithm for analysis of pulse-grams with automated output is depicted in figure 20.

**Table 3**
Intervals $A_{min}...A_{max}$ of the analysis criteria of pulsegrams.

| | Pulse type | | | | | |
|---|---|---|---|---|---|---|
| Features of PPP | "even" | "uneven" | "slow" | "fast" | "high" | "low" |
| Fractal dimension, D | 36.5302 … 39.1176 | 35.000 … 36.1376 | 31.9527 … 34.7889 | 45.0995 … 48.0018 | 50.7214 … 54.9780 | 19.2844 … 25.7860 |
| Degree of chaos, Sh | 0.5901 … 0.6345 | 2.2201 … 2.5924 | 1.0198 … 1.0931 | 1.4187 … 1.6980 | 0.4924 … 0.5605 | 0.8001 … 0.9201 |
| Area, S | 659890… … 670000 | 685140… … 701640 | 711620… … 726770 | 634990… … 657740 | 705010… … 710170 | 774700… … 784520 |

**Table 4**
Confidence intervals $A_{min}...A_{max}$ of the analysis criteria of pulsegrams.

| | Pulse type | | | | | |
|---|---|---|---|---|---|---|
| Features of PPP | "even" | "uneven" | "slow" | "fast" | "high" | "low" |
| Fractal dimension, D | 36.982 … 38.408 | 35.0305 … 35.5603 | 32.6885 … 34.2205 | 46.1923 … 47.8966 | 51.4784 … 54.0777 | 21.6591 … 24.6942 |
| Degree of chaos, Sh | 0.6051 … 0.6282 | 2.3939 … 2.5667 | 1.0652 … 1.0442 | 1.4414 … 1.5826 | 0.5125 … 0.5484 | 0.8392 … 0.8971 |
| Area, S | 661979.9 … 667318.1 | 691490.1 … 699595.9 | 713815.7 … 720942.3 | 640308.4 … 652081.6 | 705765.9 … 708442.15 | 777339.8 … 783206.2 |

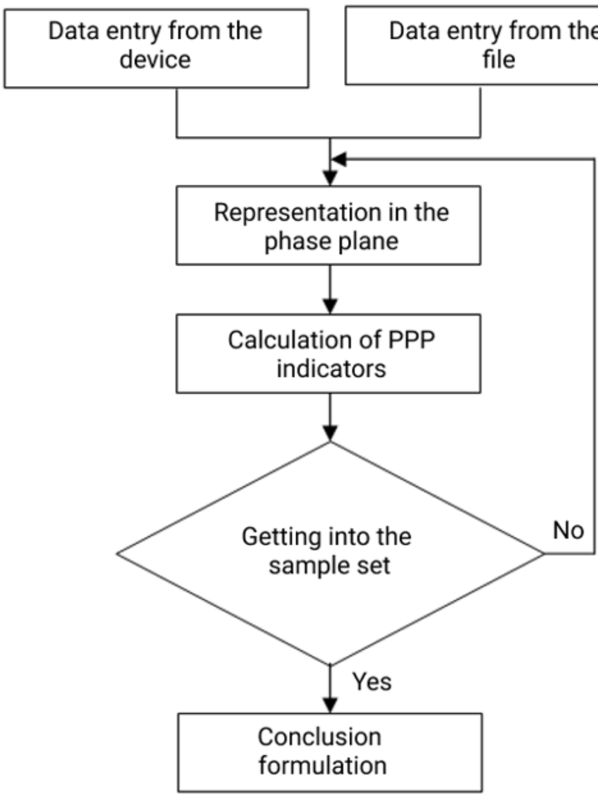


**Figure 20:** Algorithm for analysis of pulsograms with automated output.

## 5. Conclusions

When researching the pulse signal, it is often necessary to calculate a large number of concomitant parameters that can provide information about the state of the cardiovascular system and the body as a whole. To calculate these parameters, it is necessary to have mathematical and physical relationships between specific indicators of the circulatory system. Substantiation of such relationships and dependencies is contained in biophysical models of blood circulation.

In this study, the feasibility of using a refined harmonic model of the pulse wave is substantiated, which is entrusted to the study of the possibility of rapid diagnosis of the cardiovascular system. We also propose a classification of pulseograms based on the variability of pulseogram characteristics throughout the diagnostic procedure.

Based on the study, six functional sets are formed. Each of them contains an array of values from the analysis criteria – numerical characteristics of phase portraits of pulse-grams. These characteristics correspond to a particular pulse type, which will help to detect various pulse-grams, as well as diagnose the cardiovascular system for lack of dysfunction. The algorithm for analyzing pulseograms with automated conclusion is proposed and considered in detail.

The future biotechnical system that will be developed based on this model of pulsograms will be a type of edge device. This system will promote carrying out express organism diagnostics on pulse signals and also will transfer results to the server of the remote diagnostic center.

## References


[1] Abakumov, M.V., Gavrylyuk, K.V., Esikova, N.V., Lukshin, A.V., Mukhin, S.I., Sosnin, N.V., Tishkin, V.F. and Favorski, A.P., 1997. A mathematical model of the hemodynamics of a cardio-vascular system. *Differential Equations*, 33(7), pp.895–901. Available from: http://mi.mathnet.ru/de9478.

[2] Blagitko, B.Y., Zayachuk, I.M., Trach, B.M. and Pirogov, O.W., 2007. Mathematical model of pulse wave propagation in large blood vessels in sports practice. *Theory and methods of physical education*, 8(34), pp.34–36.

[3] Gnilitskyy, V.V. and Muzhitska, N.V., 2010. Refinement of the harmonic model of pulse wave for the express-diagnosis of pulsogram. *"The Journal of Zhytomyr State Technological University" / Engineering*, ((4(55)), pp.28–38. Available from: http://vtn.ztu.edu.ua/article/view/70430.

[4] Krishnasamy, E., Varrette, S. and Mucciardi, M., 2020. Edge Computing: An Overview of Framework and Application. *PRACE Technical Report*, pp.1–21. Available from: https://prace-ri.eu/wp-content/uploads/Edge-Computing-An-Overview-of-Framework-and-Applications.pdf.

[5] Muzhitskaya, N.V., 2012. *Express-diagnosis based on discrete wavelet analysis of pulse waves.* Ph.D. thesis. Zhytomyr State Technological University. Available from: https://nrat.ukrintei.ua/searchdoc/0412U000930.

[6] Nan, Y., Li, W., Deng, S. and Zomaya, A.Y., 2020. Smart healthcare systems enabled by edge computing. *Edge Computing: Models, technologies and applications.* IET Digital Library, pp.337–356. Available from: https://doi.org/10.1049/PBPC033E.

[7] Nikitchuk, T., 2015. Devising an information system for the analysis of pulse signals. *Eastern-European Journal of Enterprise Technologies*, 5(9), pp.19–23. Available from: https://doi.org/10.15587/1729-4061.2015.51219.

[8] Nikitchuk, T.M., Vakaliuk, T.A., Andreiev, O.V., Korenivska, O.L., Osadchyi, V.V. and Medvediev, M.G., 2022. Mathematical model of the base unit of the biotechnical system as

a type of edge devices. *Journal of Physics: Conference Series*, 2288(1), p.012004. Available from: https://doi.org/10.1088/1742-6596/2288/1/012004.

[9] Nikitchuk, T.M., Vakaliuk, T.A., Chernysh, O.A., Korenivska, O.L., Martseva, L.A. and Osadchyi, V.V., 2021. Architecture for edge devices for diagnostics of students' physical condition. In: S.O. Semerikov, ed. *Joint Proceedings of the Workshops on Quantum Information Technologies and Edge Computing (QuaInT+doors 2021), Zhytomyr, Ukraine, April 11, 2021*. CEUR-WS.org, *CEUR Workshop Proceedings*, vol. 2850, pp.45–56. Available from: http://ceur-ws.org/Vol-2850/paper3.pdf.

[10] Pazienza, A., Mallardi, G., Fasciano, C. and Vitulano, F., 2019. Artificial Intelligence on Edge Computing: a Healthcare Scenario in Ambient Assisted Living. In: S. Bandini, G. Cortellessa and F. Palumbo, eds. *Proceedings of the 5th Italian Workshop on Artificial Intelligence for Ambient Assisted Living 2019, co-located with 18th International Conference of the Italian Association for Artificial Intelligence, AI*AAL@AI*IA 2019, Rende, Italy, November 22, 2019*. CEUR-WS.org, *CEUR Workshop Proceedings*, vol. 2559, pp.22–37. Available from: https://ceur-ws.org/Vol-2559/paper2.pdf.

[11] Quy, V.K., Hau, N.V., Anh, D.V. and Ngoc, L.A., 2022. Smart healthcare IoT applications based on fog computing: architecture, applications and challenges. *Complex & intelligent systems*, 8(5), pp.3805–3815. Available from: https://doi.org/10.1007/s40747-021-00582-9.